Journal of Photochemistry & Photobiology, B: Biology 158 (2016) 219–227

Contents lists available at ScienceDirect

Journal of Photochemistry & Photobiology, B: Biology

journal homepage: www.elsevier.com/locate/jphotobiol

Synthesis, characterization, crystal structure, DNA and BSA binding, molecular docking and *in vitro* anticancer activities of a mononuclear dioxido-uranium(VI) complex derived from a tridentate ONO aroylhydrazone

Maryam Mohamadi [a,b], S. Yousef Ebrahimipour [a,*], Jesus Castro [c], Masoud Torkzadeh-Mahani [d]

[a] Department of Chemistry, Faculty of Science, Shahid Bahonar University of Kerman, Kerman, Iran
[b] Department of Chemistry, Payame Noor University (PNU), 19395-4697 Tehran, Iran
[c] Departamento de Química Inorgánica, Universidade de Vigo, Facultade de Química, Edificio de Ciencias Experimentais, 36310 Vigo, Galicia, Spain
[d] Department of Biotechnology, Institute of Science, High Technology and Environmental Science, Graduate University of Advance Technology, Kerman, Iran

ARTICLE INFO

Article history:
Received 31 May 2015
Received in revised form 29 February 2016
Accepted 1 March 2016
Available online 4 March 2016

Keywords:
U(VI) complex
X-ray crystal structure
DNA binding
BSA interaction
Molecular docking
MTT assays

ABSTRACT

A mononuclear dioxido-uranium(IV) complex $[UO_2(L)(DMSO)_2]$, was prepared from the reaction of (2-hydroxy-3-methoxybenzylidene)benzohydrazide [HL] with $UO_2(OAc)_2 \cdot 2H_2O$ in DMSO. The obtained complex was fully characterized. Single crystal X-ray diffraction analysis of $[UO_2(L)(DMSO)_2]$ revealed that U(VI) ion has been coordinated by ONO donor atoms of the dianionic ligand (L^{2-}), oxo groups and two DMSO molecules in a pentagonal bipyramid geometry. In addition, interactions of the complex with salmon sperm DNA and bovine serum albumin (BSA) were thoroughly investigated using UV–vis absorption, voltammetry and molecular docking methods. The experimental studies showed an intercalative mode of interaction between the complex and DNA. Experiments on BSA interaction indicated a change in the polarity of the environment surrounded the complex as a result of the interaction between BSA and $[UO_2(L)(DMSO)_2]$. Finally, MTT assays indicated that the U(VI) complex had excellent cytotoxicity against human carcinoma cell lines of MCF-7, HPG-2, and HT-29, with IC_{50} values of 8.4, 10.6 and 10.0 μM, respectively.

1. Introduction

Schiff bases are versatile ligands widely used in coordination chemistry due to their unique properties such as stability, multidenticity and easy synthesis [1]. Among these compounds, hydrazones have attracted considerable attention not only because of their variety of structure, but also for their various biological and chemical applications [2]. They have the ability to form complexes with metal ions in different oxidation states [3].

Coordination chemistry of *f*-elements is rapidly developed because their complexes show unique luminescent and magnetic properties including relevance to luminescent systems with long lifetimes, photostability and line-like emission bands [4] which make them appropriate options as diagnostic tools in biological sciences. For example, these compounds have been used as markers for immunofluorescent assays or paramagnetic contrast agents in magnetic resonance imaging [5], second-order nonlinear optical (NLO) chromophores [6–7] as well as practical reprocessing of nuclear wastes [8]. Among *f*-elements, uranium is particularly interesting since it exhibits both heavy metal and radioactive properties [9–10]. Uranium is the heaviest naturally occurring earth element with several oxidation states of II, III, IV, V, and VI [11].

Under physiological conditions, U(VI) is the most stable oxidation state of uranium [12]. Hexavalent uranium has been reported to form complexes with serum proteins, including albumin and transferrin [11,13–15]. Accordingly, investigation of the interaction between U(VI) compounds and serum proteins is of high importance with respect to the coordination chemistry of U(VI) [16], nature of the proteins [17] and quantitative description of the interaction [18].

In spite of the rapid development of novel anticancer drugs, drug resistance and undesirable side effects have created many problems in cancer therapy [19]. Thus it is necessary to identify new compounds with better properties in this regard [20].

Generally, molecules which interact with DNA affect DNA replication and transcription and ultimately, induce cell death and apoptosis. So, study of the interaction mode and mechanism of such compounds is of importance which helps us to provide new and even more efficient anticancer drugs [21].

Two broad classes of non-covalent DNA-binding agents have been identified: the intercalators and the groove binders. The intercalators

* Corresponding author at: Department of Chemistry, Shahid Bahonar University of Kerman, 76169-14111 Kerman, Iran.
E-mail addresses: Ebrahimipour@uk.ac.ir, Ebrahimipour@ymail.com (S.Y. Ebrahimipour).

http://dx.doi.org/10.1016/j.jphotobiol.2016.03.001
1011-1344/

bind via inserting a planar aromatic chromophore between adjacent base pairs of DNA, whereas the groove binders fit into the DNA minor grooves causing a little perturbation of the DNA Structure [22].

Herein, we have synthesized and fully characterized a new U(VI) complex containing a tridentate ONO aroylhydrazone Schiff base. In addition, the interaction of this complex with salmon sperm DNA and BSA have been studied using spectroscopic and electrochemical techniques. Finally, anticancer properties of the title complex against three cancer cell line of MCF-7, HT-29 and HPG-2 have been evaluated with MTT assay.

2. Experimental

2.1. Reagents

Salmon sperm DNA was purchased from Sigma (St. Louis, USA). A 1.0 mg/mL stock solution of the DNA was prepared in TE buffer (pH 7.4) and kept frozen. The concentration of the solution was determined using the molar extinction coefficient of DNA bases at 260 nm (ε_{260}) which was found to be 6600 L mol^{-1} cm^{-1} (per P or nucleotide unit). Bovine serum albumin (BSA) was obtained from Merck (Germany). Other chemicals and solvents were of analytical reagent grade and used as received. [HL] was prepared according to previous report [23].

2.2. Instrumentation

Cyclic voltammograms were obtained using an Autolab PGSTAT 302 electrochemical system from Metrohm (Herisau, Switzerland) interfaced with a personal computer for data acquisition and potential control. Electronic spectra were recorded on a double beam UV–vis–NIR Varian Cary 500 spectrophotometer (Victoria, Australia). Micro analyses for C, H, N were performed using a Thermo Finnigan Flash Elemental Analyzer 1112EA. Melting points were Determined with the help of an Electrothermal Apparatus-9200. FT-IR spectra were recorded at a Bruker-Tensor 27 by embedding the material in KBr discs in the range of 400–4000 cm^{-1}. Molar conductance measurements were made by means of a Metrohm 712 Conductometer in DMSO. ^{1}H NMR spectra were recorded at 25 °C on AVANCE BRX 500 and 300 MHz spectrometers. Diffraction data were measured using a Bruker Smart 6000 diffractometer.

2.3. Synthesis of (2-hydroxy-3-methoxybenzylidene) benzohydrazide [HL]

A mixture of benzohydrazide (0.14 g, 1 mmol) and 3-methoxy-2-hydroxy benzaldehyde (0.15 g, 1 mmol) was refluxed in 10 mL methanol. After 1 h, the resulted precipitate was filtered, washed with cold ethanol and dried in vacuum over silica gel.

Yield: 0.22 g, 83%. m.p.: 116 °C. FT-IR (KBr), cm^{-1}: ν(NH) 3571, ν(OH) 3367, ν(CH$_{ar}$) 2839–3062, ν(C═O) 1647, ν(C═N) 1610, ν(C═C$_{ring}$) 1470, ν(N—N) 1149, ν(C—O) 1296. ^{1}H NMR (500 MHz, DMSO-d_6, 25 °C, ppm): δ = 12.10 (*s*, 1H; NH), 11.03 (*s*, 1H; OH), 8.67 (*s*, 1H; CH═N), 6.85–7.96 (*m*, 8H, rings), 3.82 (s, 3H, OCH$_3$). UV/vis (DMSO) λ_{max}, nm (logε, L mol^{-1} cm^{-1}): 307(4.61), 339(4.24), 423(2.90).

2.4. Synthesis of Bis (dimethylsulfoxide) (3-Methoxy-2-oxidobenzylidene) benzohydrazonato-dioxido-uranium(VI) [UO$_2$(L)(DMSO)$_2$]

A DMSO solution (5 mL) of HL (0.1 mmol, 0.03 g) and $UO_2(OAc)_2 \cdot 2H_2O$ (0.1 mmol, 0.042 g) was stirred at room temperature for 2 h. Suitable crystals for X-ray analysis were obtained after slow evaporation of the solution for 5 days. The obtained crystals were filtered off and dried in a desiccator over silica gel.

Yield: 0.042 g, 60%. m.p.:>300 °C. Anal. Calc. for $C_{19}H_{24}N_2O_7S_2U$ (694.56 g mol^{-1}): C, 32.86; H, 3.48; N, 4.03. Found: C, 32.82; H, 3.79; N, 4.14%. Molar conductance (10^{-3} M, DMSO) 3.7 Ω^{-1} cm^2 mol^{-1}. FT-IR (KBr), cm^{-1}: ν(CH) 2837–3059, ν(C═N) 1595, ν(C═C$_{ring}$) 1461, ν(C—O) 1243, ν(NN) 1142, δ_{oopb}(CH) 712, ν(S═O) 1012, ν_{asy}(*trans*-UO_2) 949, ν_{sy}(*trans*-UO_2) 891, ν(CSC) 639, ν(U—O) 533, ν(U—N) 470. ^{1}H NMR (300 MHz, DMSO-d_6, 25 °C, ppm): δ = 9.24 (*s*, 1H; CH═N), 6.61–8.38 (*m*, 8H, rings), 3.94 (s, 3H, OCH$_3$), 3.36 (s, 6H, S(CH$_3$)$_2$). UV/vis (DMSO) λ_{max}, nm (logε, L mol^{-1} cm^{-1}): 286 (4.14), 347 (4.16), 380 (4.45), 405 (4.34).

2.5. Crystal Structure Determination

Crystallographic data were collected at room temperature using a Bruker Smart 6000 CCD detector and Cu-Kα radiation (λ = 1.54178 Å) generated by an Incoatec microfocus source equipped with Incoatec Quazar MX optics. The software APEX2 was used for collecting frames of data, indexing reflections, and the determination of lattice parameters, SAINT for integration of intensity of reflections, and SADABS for scaling and empirical absorption correction [24].

Crystallographic treatment was performed with the Oscail program [25]. The crystal structure was solved with direct methods and refined using a full-matrix least-squares method based on F^2 [26]. Non-hydrogen atoms were refined with anisotropic displacement parameters. Hydrogen atoms were included in idealized positions and refined with isotropic displacement parameters. It was found that one of the DMSO molecules bonded to the uranium metal was disordered and occupancy factors of 0.866(5):0.134(5) were refined for two sulfur atoms. Details of crystal data and structural refinement are given in Table 1.

2.6. UV–Vis Absorption Studies

Interaction of the U(VI) complex with DNA has been studied with UV spectroscopy in order to investigate the possible binding mode.

Table 1
Crystal data and structure refinement for [UO$_2$(L)(DMSO)$_2$].

Empirical formula	$C_{19}H_{24}N_2O_7S_2U$
Formula weight	694.55
Temperature	296(2) K
Wavelength	1.54178 Å
Crystal system	Monoclinic
Space group	$P2_1/c$
Unit cell dimensions	a = 15.5721(8) Å b = 10.1274(5) Å c = 16.7245(8) Å α = 90° β = 115.5819(12)° γ = 90°
Volume	2379.0(2) Å^3
Z	4
Density (calculated)	1.939 Mg/m^3
Absorption coefficient	21.209 mm^{-1}
F(000)	1328
Crystal size	0.166 × 0.101 × 0.067 mm
Theta range for data collection	3.15 to 67.84 °.
Index ranges	−18 ≤ h ≤ 18 −12 ≤ k ≤ 12 −19 ≤ l ≤ 19
Reflections collected	62,993
Independent reflections	4288 [R(int) = 0.0582]
Reflections observed (>2σ)	4128
Data Completeness	0.994
Absorption correction	Semi-empirical from equivalents
Max. and min. Transmission	0.7530 and 0.2427
Refinement method	Full-matrix least-squares on F^2
Data/restraints/parameters	4288/0/295
Goodness-of-fit on F^2	1.048
Final R indices [I > 2σ(I)]	R_1 = 0.0246 wR_2 = 0.0667
R indices (all data)	R_1 = 0.0253 wR_2 = 0.0678
Largest diff. peak and hole	2.021 and −0.872 e·Å^{-3}

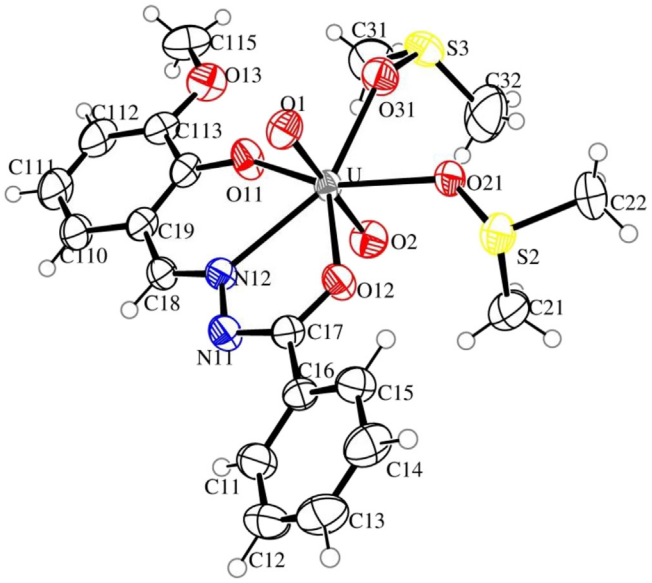

Fig. 1. ORTEP (30% probability level) drawn of $[UO_2(L)(DMSO)_2]$. Atom S3 is disorder over to positions, with occupancy factors of 0.866(5):0.134(5). Last one was not drawn.

Absorption titration of DNA with the complex was carried out using fixed concentration of DNA (4.5×10^{-5} M) in 0.02 M PBS (pH = 7.4) while the concentration of the complex was gradually increased. In the absorption titration of the complex with DNA, the UV–vis spectra of the complex (6.0×10^{-5} M in PBS) in the presence of varying concentrations of DNA were recorded.

All experiments were carried out at room temperature. In all experiments, the incubation time for equilibrating the interaction was 5 min.

2.7. Cyclic Voltammetric Measurements

Electrochemical techniques can be employed to study the interaction of electro-active complexes with DNA in order to confirm the binding mode suggested by spectroscopic studies [27]. Cyclic voltammograms of $[UO_2(L)(DMSO)_2]$ were recorded before and after adding DNA to a fixed concentration of the complex in 0.1 M PBS at the scan rate of 100 mV/s.

2.8. Cell Proliferation and Viability Assay

Toxicity of the synthesized hydrazone ligand [HL] and its U(VI) complex against three human carcinoma cell lines namely HPG-2, HT-29 and MCF-7 was investigated using MTT assay. MTT is transformed into formazan by the enzyme hydrogenase in mitochondria. The surviving cells can be determined by measuring their ability to reduce MTT (yellow) to formazan product (purple). Cytotoxicity of the synthesized

Table 2
Selected bond lengths [Å] and angles [°] for $[UO_2(L)(DMSO)_2]$.

U–O(1)	1.778(3)	U–O(2)	1.780(3)
U–O(11)	2.210(3)	U–O(12)	2.333(3)
U–O(31)	2.402(3)	U–O(21)	2.438(3)
U–N(12)	2.568(4)		
O(1)–U–O(2)	179.62(17)	O(12)–U–N(12)	63.03(10)
O(11)–U–N(12)	70.25(11)	O(12)–U–O(21)	71.13(11)
O(31)–U–O(21)	73.70(12)	O(11)–U–O(31)	82.75(13)
O(1)–U–O(11)	92.05(15)	O(2)–U–O(11)	88.02(16)
O(1)–U–O(12)	89.52(14)	O(2)–U–O(12)	90.16(14)
O(1)–U–O(31)	85.17(14)	O(2)–U–O(31)	95.21(15)
O(1)–U–O(21)	94.20(14)	O(2)–U–O(21)	85.89(15)
O(1)–U–N(12)	88.29(14)	O(2)–U–N(12)	91.38(15)

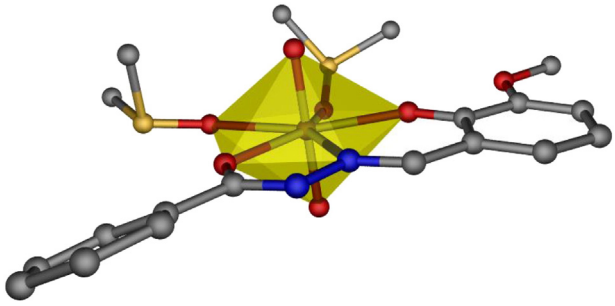

Fig. 2. View of the twisting of the hydrazone ligand in $[UO_2(L)(DMSO)_2]$.

compounds against each cell line can be concluded from dose–response curves.

The cells were placed in 96-well micro-assay culture plates at a density of 5×10^3 cells per well and grown at 37 °C in a humidified 5% CO_2 incubator for 24 h. Then the cells were treated with varying concentrations of the complex and ligand (0.31, 0.62, 1.25, 2.5, 5, 10, 20 and 40 μM) for 24 h. After that, 20 μL of MTT solution was added to each plate and incubation was performed at 37 °C for 4 h. The metabolically active cells reduced MTT to blue formazan crystals. The crystals formed were then solubilized upon addition of DMSO and incubated at room temperature for 20 min. Finally, absorbance (A) of the solution of each well was measured with ELISA reader at 545 nm. The absorbance was then converted to percentage of cell-growth inhibition according to the following formula:

$$\%\text{Cell cytotoxicity} = \left[1-\left(A_{drug}/A_{control}\right)\right] \times 100.$$

IC_{50} value defined as the compound concentration required reducing the survival of cells by 50%, was also calculated.

2.9. Molecular Docking

Molecular docking is a powerful technique to predict the binding affinity and orientation of different drugs to their bio-targets such as proteins and DNA. In the present study, molecular docking was used to investigate the binding mode and intermolecular interaction of $[UO_2(L)(DMSO)_2]$ with DNA and BSA. Coordination sphere of the U(VI) complex was generated from its X-ray crystal structure as a CIF file. The CIF file was then converted to PDB format using Mercury software (http://www.ccdc.cam.ac.uk/). The molecular docking study was carried out using Autodock Vina software [28]. All molecular images and animations were produced using Discovery Studio Visualizer 4.1 package.

2.10. Chemical Structures of DNA and BSA

The initial structure of BSA was taken from the Protein Data Bank (PDB ID: 4F5S) at a resolution of 2.47 Å. Also, the DNA sequence $d(CGCGAATTCGCG)_2$ was obtained from the Protein Data Bank (PDB ID: 1BNA) at a resolution of 1.90 Å.

Table 3
Hydrogen bonds for $[UO_2(L)(DMSO)_2]$.

D–H…A	d(D–H)	d(H…A)	d(D…A)	<(DHA)
C(115)–H(11C)…O(2^{i})	0.96	2.57	3.489(7)	159.3
C(32)–H(32B)…N(11^{ii})	0.96	2.57	3.467(9)	155.5

Symmetry transformations used to generate equivalent atoms:
i, x, 3/2-y,z + 1/2; ii, x, y + 1, z.

Table 4
Summary of C–H···π interaction parameters, [Å] and [°].

Interaction (*)	H…Cg [Å]	H-Perp [Å]	γ	X–H… Cg	X…Cg [Å]	X–H···π
C(12)–H(12)···Ct1[a]	2.89	2.72	20.02	162	3.791(6)	65

(*) Code: Symmetry operations: a, x, 1/2-y, z-1/2; H-Perp, perpendicular distance of H to ring plane; γ, angle between Ct-H vector and ring normal; X–H···π, angle of the X–H bond with the π-plane.

3. Results and Discussions

The title complex was prepared from the reaction of the aroylhydrazone Schiff base ligand (HL) and $UO_2(OAc)_2.2H_2O$ at 1:1 M ratio. The complex was found to be stable in air and soluble in DMSO and DMF while less soluble in methanol, chloroform, and acetonitrile and insoluble in *n*-hexane and diethyl ether. Molar conductivity value of the U(VI) complex was equal to 3.7 Ω^1 cm^2 mol^1 in DMSO, indicating the non-electrolytic behavior of this complex.

3.1. Spectral Characterization

FT-IR spectrum of HL (Fig. S1) showed OH and NH vibrations at 3571 and 3367 cm^{-1} which were disappeared in the U(VI) complex (Fig. S2) indicating that the *enolic* form of the ligand participates in the complexation process [23]. Also, a 15-cm^{-1} red shift was observed in the azomethine stretching vibration of the complex compared with that of the free ligand HL which reveals the coordination takes place through azomethine nitrogen [29–30]. In the $[UO_2(L)(DMSO)]$ spectrum, CO vibration also shifted to lower frequencies supporting that the phenolic oxygen contributes in the complexation [31]. The asymmetric and symmetric vibrations of *trans*-UO_2 were appeared at 949 and 891 cm^{-1}, respectively [32].

The ^1H NMR spectrum of $[UO_2(L)(DMSO)]$ in DMSO is presented in Fig. S4 and its spectral data are listed in the experimental section. In the spectrum of the U(VI) complex, the methine proton is observed at 9.2 ppm which is at lower filed than that of its Schiff base ligand [HL] (Fig. S3), indicating the coordination of the azomethine nitrogen to the metal center. Protons of the aromatic rings are located in the range of 6.6–8.4 ppm as multiplet signals. The singlet signal appeared at 3.9 ppm corresponds to the protons of the methoxy group [23].

Electronic spectra of HL and its U(VI) complex have been recorded in DMSO. In the spectrum of the ligand, the absorption bands related to n→ π* and π → π* transitions of the azomethine moiety, and aromatic rings of the hydrazone ligand were located between 307 nm and 423 nm [33]. For the U(VI) complex, these intra-ligand transitions showed some shifts compared with the transitions of free ONO ligand, indicating enolization of the ligand followed by its deprotonation. In the spectrum of the complex, absorption bands of the ligand-to-metal charge transfer (LMCT) assigned to N → M and O → M transitions were observed at 380 nm (4.45) and 430 nm (4.34), respectively [32].

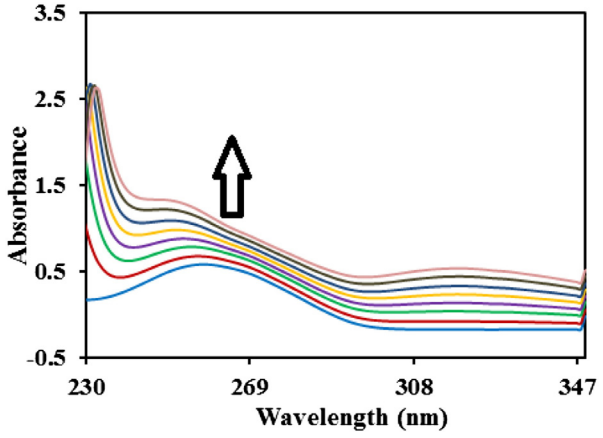

Fig. 3. Electronic absorption spectra obtained from the titration of 4.5×10^{-5} M salmon sperm DNA in 20 mM PBS (pH 7.4) with increasing amounts of $[UO_2(L)(DMSO)_2]$ (0, 9.4, 18.8, 28.2, 37.6, 47.1, 56.5 and 65.9 μM respectively from down to up).

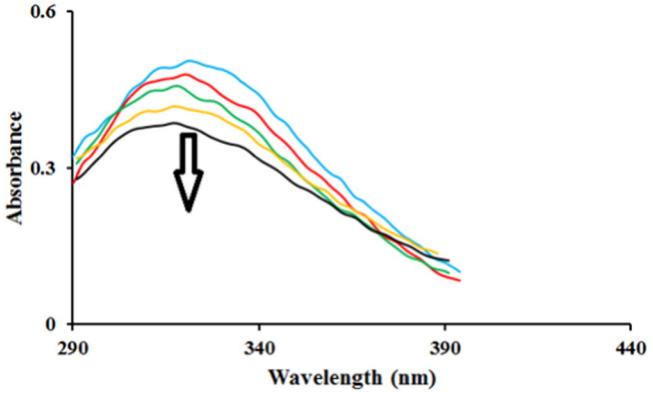

Fig. 4. Electronic absorption spectra obtained from the titration of 6.0×10^{-5} M $[UO_2(L)(DMSO)_2]$ in 20 mM PBS (pH 7.4) with increasing amounts of salmon sperm DNA (0, 3.0×10^{-5}, 1.3×10^{-4}, 5.0×10^{-4} and 2.0×10^{-3}, respectively from up to down).

3.2. X-ray Crystal Structure

Compound $[UO_2(L)(DMSO)_2]$ consists of an uranium(VI) ion coordinated by a tridentated dianionic (3-methoxy-2-oxidobenzylidene) benzohydrazonato ligand (L^{2-}), two oxo groups and two molecules of dimethylsulfoxide leading a pentagonal bipyramid environment for the actinide metal. ORTEP drawn of the compound is depicted in Fig. 1 along with the labeling scheme, and selected bond lengths. Also, corresponding angles are set out in Table 2.

Disposition of oxo groups are *trans*, with an O–U–O angle of 179.62(17)°, as is usual for the so-called uranyl compounds [UO_2^{2+}] [34–37]. Sum of the angles in the equatorial plane was 360.86°. However, this value cannot be used as a probe of the planarity since oxygen atoms from DMSO ligands are clearly deviated, one 0.140(2) below and the other 0.167(2) over the plane (with a root-mean-square deviation from a plane of 0.123 Å), in such a way that if the most deviated atom is eliminated from the calculations, the best fitted plane, formed by O(11), O(12), O(21) and N(12) (root-mean-square deviation value of 0.003 Å) leaves the O(31) atom at 0.459(6) Å and the Uranium atom at 0.094(2) Å. A three-fused system is found in the complex structure, the methoxyphenolate ring and two metallacycles, one of them is six-membered and the other is five-membered. The metallacycles form dihedral angles of 4.2(3)° and 1.9(3)°, respectively for the six- and five-

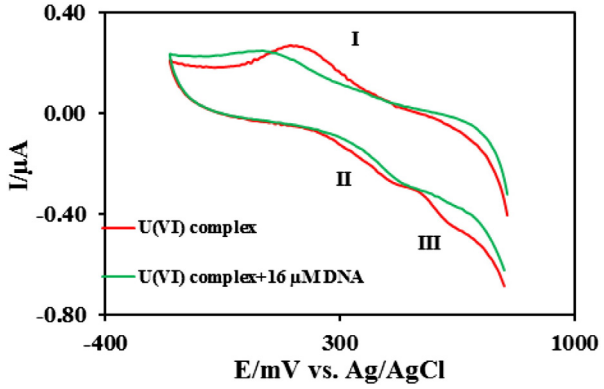

Fig. 5. Cyclic voltammograms of $[UO_2(L)(DMSO)_2]$ and $[UO_2(L)(DMSO)_2]$-DNA adduct at the scan rate of 100 mV/s.

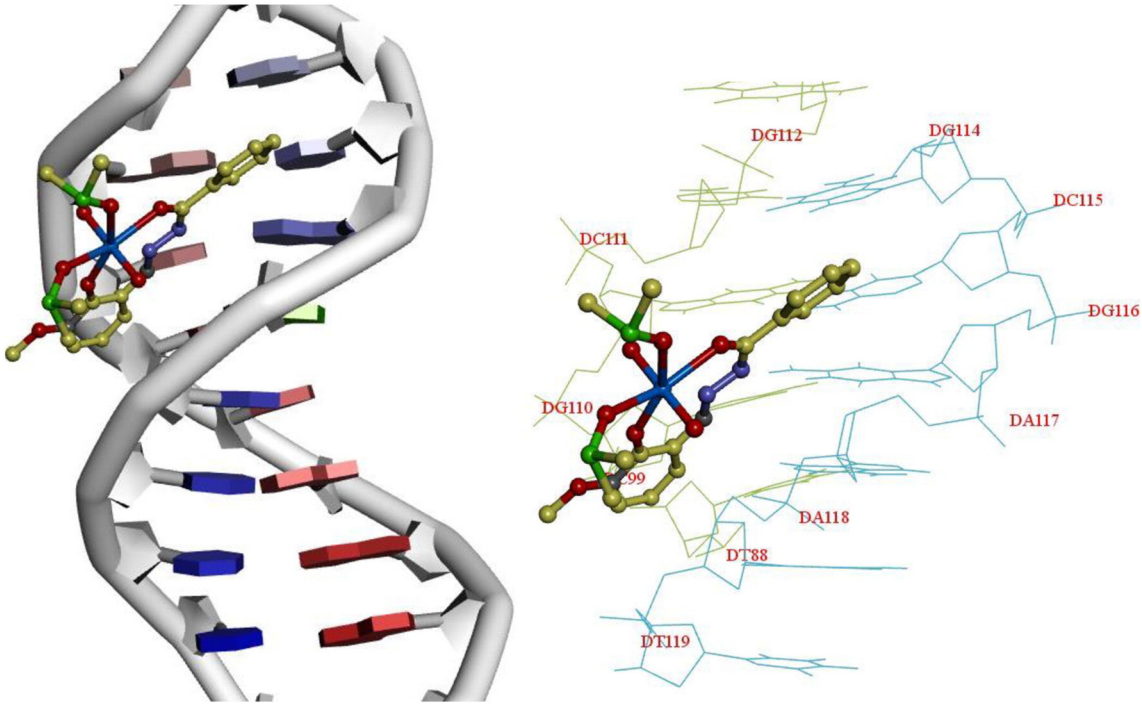

Fig. 6. Molecular docking perspective of the U(VI) complex with DNA (left) three-dimensional interactions generated by Discovery Studio 4.1 (right).

membered rings The planarity of the three-fused system is such that the root-mean-square deviation for the best plane (13 atoms including uranium) is 0.0507 Å. The phenyl ring on the carbohydrazone is, however, twisted 22.4(2)° (dihedral angle between the planes) due to the free rotation of the C(16)-C(17) bond (Fig. 2). The pentagonal bipyramid polyhedron around the metal is also distorted due to the presence of the five-membered metala-ring with a chelate angle of 63.0(1)° while the six-membered metala-ring produces a chelate angle of 70.3(1)°. The other *cis* angles in the equatorial plane are, 71.1(1), 73.7(1) and 82.7(1)°, where the differences can be due to the sterical requirements of the DMSO ligand. The bond distances in the uranyl group [UO_2^{2+}] are 1.778(3) and 1.780(3) Å which are slightly longer than those found for the binuclear compound [$(UO_2)_2(H_6pyr_2oxdihyd)(DMSO)_4$] [37], 1.778(7) and 1.766(7) Å. However, the U—O (from DMSO) bond distances are longer than those of similar compounds [2.402(3) and 2.438(3) Å vs. 2.387(7) and 2.391(7) Å]. A similar U–O distance of 2.395(3) Å was reported in [2-({(ethylsulfanyl)[2-(2-oxidobenzylidene)hydrazinylidene]methyl}iminomethyl)phenolato] dioxidouranium(VI) [35]. Coordination of the aroylhydrazone ligand can be compared with the binuclear compound [$(UO_2)_2(H_6pyr_2oxdihyd)(DMSO)_4$] [37], a compound with two pentagonal bipyramid uranium atoms in an NO_6 environment, where the nitrogen atom belongs to a hydrazone ligand resulted in similar bond distances in the complex structure. Other uranyl complexes with salicylaldehyde benzoylhydrazone described in the literature [36] contain monodeprotonated ligands, so the lengths of their U—O bonds are not comparable with the complex synthesized here.

Some non-classical hydrogen interactions, C—H···X (X═N,O) construct the supramolecular network. The C(115)···O(2^{i}) interactions lead to the growth of the crystal in the *c* axis, while the C(32)···N(11^{ii}) ones result in the growth of the crystal in the *b* axis. The parameters of these interactions are given in Table 3, Figs. S5 and S6. There are also a CH···π interaction (Table 4) that reinforce the growth in the *c* axis as is show in Fig. S7. A presentation of the unit cell is shown in Fig. S8.

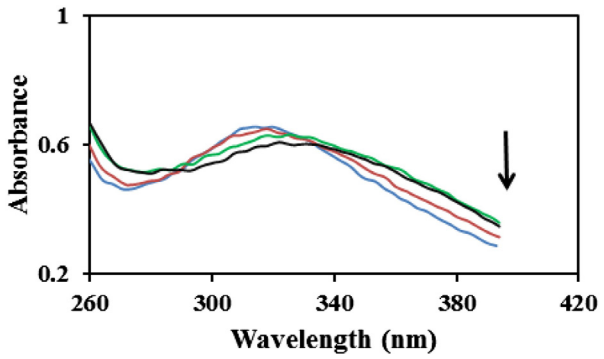

Fig. 7. Electronic absorption spectra obtained from the titration of 3.0×10^{-5} M [UO_2(L)(DMSO)$_2$] in PBS (pH 7.4) in the absence and presence of increasing concentrations of BSA.

3.3. Absorption Titration of DNA With the Complex

As Fig. 3 shows, a broad band is observed in the UV spectrum of DNA with a maximum (λ_{max}) placed at about 260 nm corresponding to purine and pyrimidine bases of DNA [38]. Upon addition of varying concentrations of the synthesized U(VI) complex to the DNA solution, the intensity of the absorption band shows a significant increase with a red shift of 7 nm in the λ_{max}.

This observation exhibits that purine and pyrimidine bases of DNA have been exposed due to the binding of the complex to DNA. So, an intercalation interaction of the complex through the stacking interaction of the aromatic rings of the ligand HL and the base pairs of DNA is proposed [39]. On the other words, interaction between the complex and DNA causes some changes in the conformation of DNA [40].

3.4. Absorption Titration of the Complex with DNA

Interaction of metal complexes with DNA leads to electronic perturbations in the complexes, so electronic absorption spectroscopy can be used to investigate the interaction characteristics [41].

The absorption spectra of the U(VI) complex in the absence and presence of varying concentrations of DNA are given in Fig. 4. As is seen, the complex exhibits a broad absorption band at about 320 nm

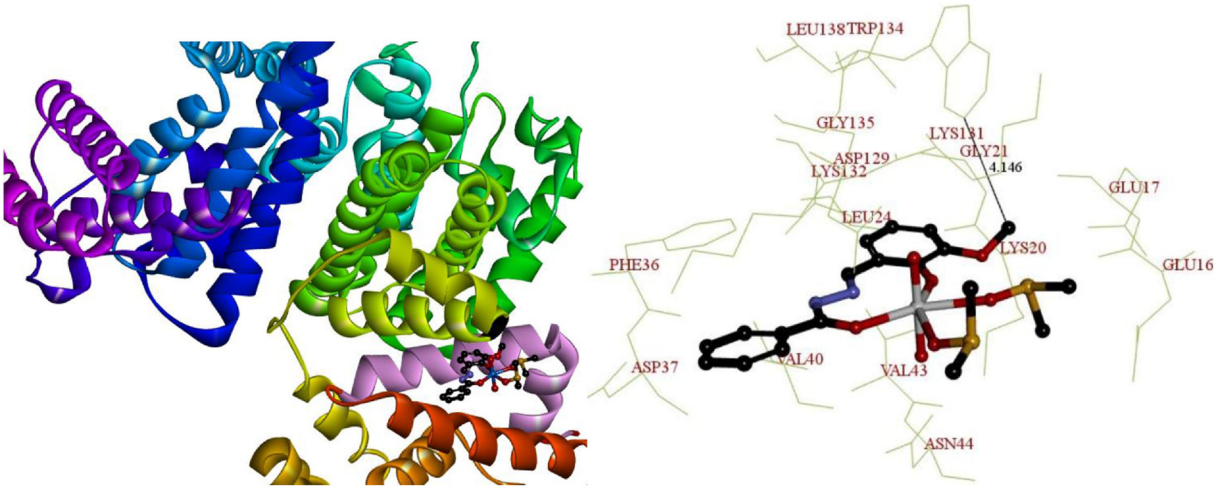

Fig. 8. A molecular docking perspective of $[UO_2(L)(DMSO)]$with BSA (left) and Three-dimensional interactions generated by Discovery Studio 4.1 (right).

with $\varepsilon = 8.4 \times 10^3\ cm^{-1}\ M^{-1}$ assigned to the π–π* transition of the aromatic chromophore. When titrated by the DNA, the intensity of the absorption peak decreases by more than 30% accompanied with a red shift of 5 nm at [DNA]/[complex] ratio of 33. These high hypochromic and bathochromic effects suggest that this complex possesses a high propensity for DNA binding. According to the spectral characteristics, an intercalative mode of interaction is suggested for the U(VI) complex-DNA system. Due to the intercalation, π* anti-bonding orbital of the complex couples with π bonding orbital of the DNA base pairs which reduces the π–π* transition energy and results in a bathochromic shift [42].

3.5. Electrochemical Studies

Cyclic voltammetry is a useful technique to study the interaction of electro-active complexes with DNA in order to confirm the DNA binding mode suggested by spectroscopic studies [43].

Cyclic voltammograms of $[UO_2(L)(DMSO)]$ in the absence and presence of DNA are depicted in Fig. 5. Cyclic voltammogram of the U(VI) complex in the absence of DNA exhibits a quasi-reversible redox behavior. In the forward wave, a peak (peak I) is observed at 0.197 V with the peak current of 0.232 μA, corresponding to U(VI)/U(IV) redox couple. In the reverse scan, two successive waves are observed at 0.458 V (peak II) and 0.620 V (peak II) with the peak currents of 0.22 μA and 0.143 μA, respectively which can be assigned to U(IV)/U(V) and U(V)/U(VI) couples.

Addition of DNA to the complex solution causes a decrease in the current of peak I by 7.7% and a negative shift in the peak potential ($E_{pc} = 0.098$ V). Furthermore, the potential of peak II (E_{pa}) shows a shift to a more positive potential (0.467 V) with a small decrease in the peak current. In addition, peak III disappears in the complex-DNA system. The observed decreases in the peak currents are related to the interaction between the $[UO_2(L)(DMSO)_2]$ complex and DNA which can be explained by the slow diffusion of the complex-DNA adduct to the electrode surface.

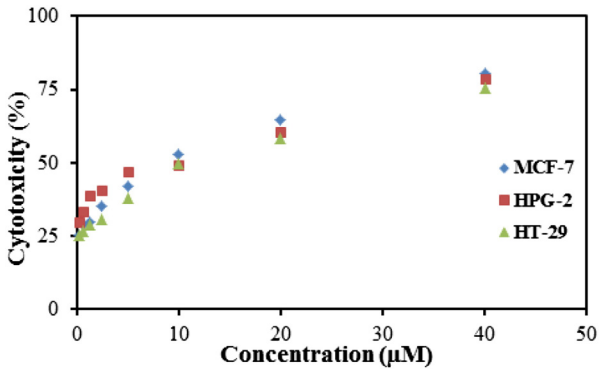

Fig. 9. Anticancer activities of different concentrations of $[UO_2(L)(DMSO)_2]$ against HPG-2, HT-29 and MCF-7 cell lines.

The interaction mode can be found from the changes of peak separation (ΔE_p) and half-wave potential ($E_{1/2}$) due to the interaction. ΔE_p and $E_{1/2}$ are defined as the difference and the average of E_{pa} and E_{pc}, respectively.

According to the obtained results, interaction with DNA decreases $E_{1/2}$ of the complex from 0.327 V to 0.282 V while increases ΔE_p from 0.261 V to 0.369 V.

Generally, if the interaction mode is of an electrostatic binding nature, the half-wave potential shifts to a more negative value, while intercalation binding results in the shift of half-wave potential to a more positive value [44]. So, electrochemical studies confirm the intercalative mode of the interaction between the title U(VI) complex and DNA which has been proposed by spectroscopic studies.

3.6. Molecular Docking of the U(VI) Complex With DNA

In order to determine the site of DNA involved in its interaction with $[UO_2(L)(DMSO)_2]$, blind docking was performed on a DNA duplex with the sequence of $d(CGCGAATTCGCG)_2$. The obtained conformations were ranked based on the lowest free binding energy. Accordingly, the most stable complex formed between the DNA and $[UO_2(L)(DMSO)_2]$ was found to possess -6.9 kcal mol^{-1} binding energy which indicates that the U(VI) complex has a good binding affinity to DNA and this binding is spontaneous. Fig. 6 depicts the energy-minimized docked pose of $[UO_2(L)(DMSO)_2]$. There are several categories of hydrophobic contacts between the complex atoms and bases of DNA, including, DT 119, DA 118, DA 117, DG 116, DC 115, DG 114, DG 112, DC 111, DG 110, DC 99 and DT 88 (Fig. 6). The resulting docking model reveals that the U(VI) complex partially intercalates into the DNA duplex through its minor groove.

3.7. BSA Interaction

3.7.1. UV–Vis Absorption Studies

BSA is an extensively studied serum albumin protein, due to its structural similarity with human serum albumin [45]. Fig. 7 shows the absorption spectra of $[UO_2(L)(DMSO)_2]$ in the presence of varying

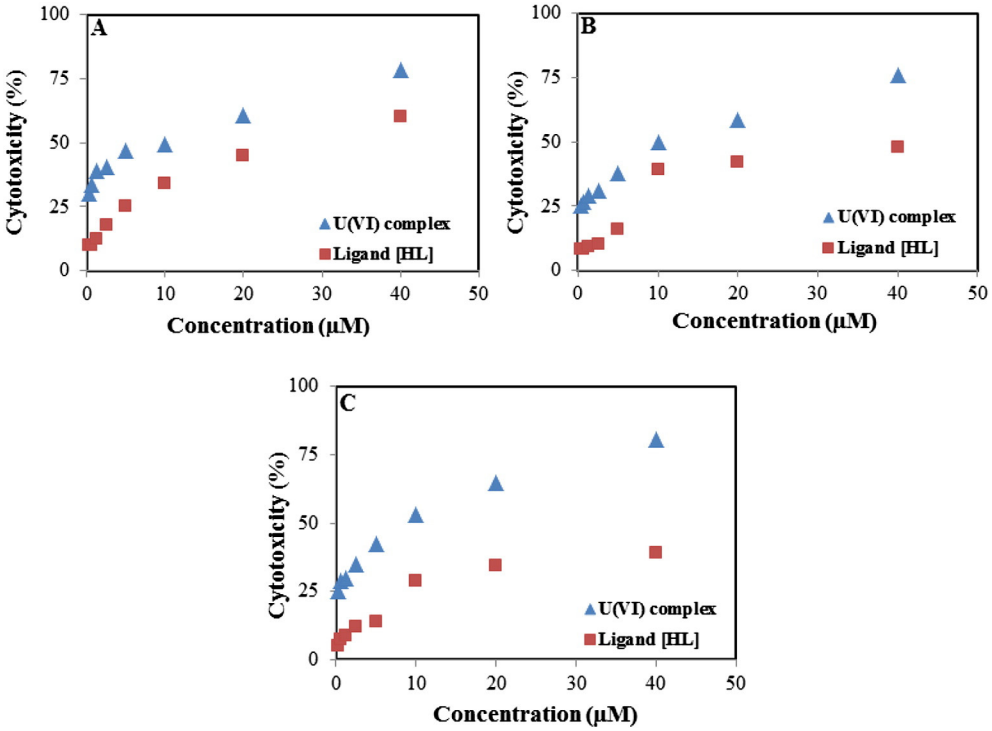

Fig. 10. Cytotoxicity percentage of $[UO_2(L)(DMSO)_2]$ and HL in the concentration range of 0.31–40 μM against HPG-2 (A), HT-29 (B) and MCF-7 (C) cell lines.

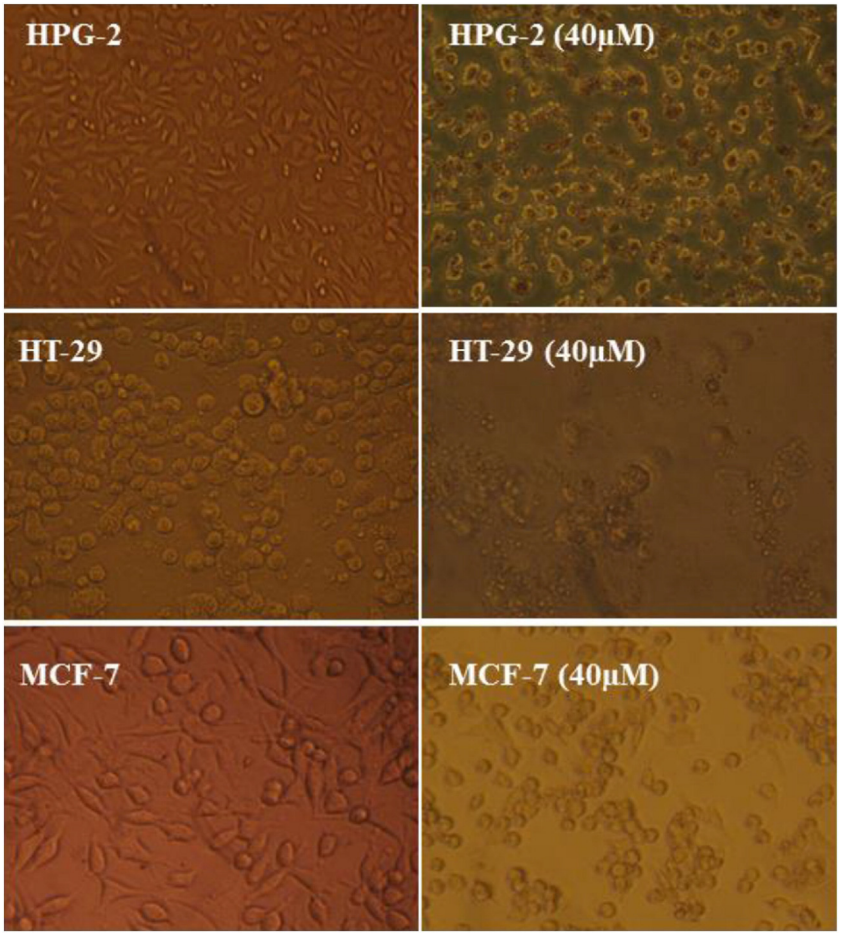

Fig. 11. Microscopic photographs of HPG-2, HT-29 and MCF-7 cancer cells in the absence and presence of 40 μM $[UO_2(L)(DMSO)_2]$.

concentrations of BSA. As can be seen, the intensity of the absorption peak of the complex observed at about 320 nm decreases with a red shift of 7 nm. These observations indicate an interaction between BSA and the title U(VI) complex resulted in some changes in the polarity of the environment surrounded the complex [46] and π–π stacking interaction between the aromatic rings of the complex and those of the aromatic amino acid residues [47].

3.7.2. Molecular Docking of the U(VI) Complex With BSA

To obtain useful information on the preferred binding location and to understand the mechanism of $[UO_2(L)(DMSO)_2]$-BSA interaction, molecular docking technique has been used to dock the complex into the protein. Two principal binding sites have been found in BSA in the proximity of Trp134 and Trp213 [48]. The probable binding poses obtained from blind docking have been ranked based on the lowest binding free energy. According to the obtained results, the title U(VI) complex prefers the binding pocket of domain I containing Trp134 with the relative binding energy of -7.1 kcal mol^1. Also, docking studies shows that the distance between Trp134 residue and the U(VI) complex is 4.146 Å. The energetically favorable docked image is shown in Fig. 8. As can be seen, there are interactions between the U(VI) complex and Leu 138, Trp 134, Gly 135, Asp 129, Lys 132, Leu 24, Val 40, Asp37, Phe 36, Lys 131, Gly 21, Glu 17, Glu 16, Val 43 and Asn 44.

3.8. Cytotoxicity Study

The synthesized Schiff base ligand and its U(VI) complex have been tested for their in-vitro anti-proliferative activity against MCF-7, HPG-2 and HT-29 cancer cell lines. Fig. 9 reveals the effect of different concentrations of [HL] ligand and $[UO_2(L)(DMSO)_2]$ on the cell lines. As is seen, the viability of all cell lines decreases in both ligand- and complex-treated ones as a function of concentration indicating a dose-dependent growth inhibitory effect. For all cell types and in all tested concentrations, it is clear that toxicity of the U(VI) complex is considerably higher than that of the ligand. Especially in low concentrations, free ligand [HL] shows less than 30% of the toxicity of $[UO_2(L)(DMSO)]$. On the other words, complexation with U(VI) significantly improves the anticancer effect of the parent ligand.

In addition, viability of MCF-7, HPG-2 and HT-29 cancer cell lines in the presence of different concentrations of the U(VI) complex has been compared and revealed in Fig. 10. As can be seen, HPG-2 is the most sensitive cell line to the complex at concentrations ≤5 μM. At higher concentrations, proliferation of MCF-7 cells is affected more than those of the other cell lines. It is worth mentioning that, at high concentrations the side effect of the compound should be also considered. Fig. 11 shows the photos taken from the cell lines before and after treating by $[UO_2(L)(DMSO)_2]$. It is clear that the complex has cytotoxicity effect against all three cell lines.

Finally, IC_{50} values for the complex against MCF-7, HPG-2 and HT-29 cell lines were calculated to be 8.4, 10.6 and 10.0 μM, respectively which are smaller than those reported for the well-known anticancer drug, *cis*-platin [49,50].

4. Conclusion

Herein, we report the synthesis and characterization of a new dioxido-uranium(IV) complex as well as the results of investigating its interaction with DNA and BSA and anticancer activity. The reaction of $UO_2(OAc)_2{\cdot}2H_2O$ and (2-hydroxy-3-methoxybenzylidene)benzohydrazide [HL] in DMSO has resulted in the formation of the complex with the formula of $[UO_2(L)(DMSO)_2]$. According to the results of X-ray crystallography, U(VI) ion has been coordinated by ONO donor atoms of the dibasic aroyl hydrazone ligand, oxo groups and two DMSO molecules in a pentagonal bipyramid geometry.

As shown by spectroscopic and electrochemical studies, the complex can intercalate into DNA duplex. The changes observed in the absorption spectrum of $[UO_2(L)(DMSO)_2]$ in the presence of BSA can be related to the interaction with BSA. Molecular docking studies on the interaction of $[UO_2(L)(DMSO)_2]$ with DNA and BSA have confirmed the experimental results. MTT assays has revealed the anticancer activity of the title complex against MCF-7, HPG-2, and HT-29, with IC_{50} values of 8.4, 10.6 and 10.0 μM, respectively.

The existing results of biological activity of the title complex as a DNA- and BSA-binding compound as well as an anticancer agent are promising and can open a new window for the use of this compound as a potential metallodrug.

Acknowledgment

We are grateful to the Shahid Bahonar University of Kerman for the financial support of this work.

Appendix A. Supplementary data

Crystallographic data for the $[UO_2(L)(DMSO)_2]$ has been deposited with the Cambridge Crystallographic Data Centre, CCDC No. 1403371. Copies of this information may be obtained from the Director, CCDC, 12 Union Road, Cambridge, CB2 1EZ, UK (fax: +44-1223-336033; e-mail: deposit@ccdc.cam.ac.uk or http://www.ccdc.cam.ac.uk). Supplementary data associated with this article can be found in the online version, at http://dx.doi.org/10.1016/j.jphotobiol.2016.03.001.

References

[1] S.Y. Ebrahimipour, I. Sheikhshoaie, A.C. Kautz, M. Ameri, H. Pasban-Aliabadi, H.A. Rudbari, G. Bruno, C. Janiak, Polyhedron 93 (2015) 99–105.
[2] I. Sheikhshoaie, S.Y. Ebrahimipour, M. Sheikhshoaie, H.A. Rudbari, M. Khaleghi, G. Bruno, Spectrochim. Acta, Part A 124 (2014) 548–555.
[3] N.A. Mangalam, S. Sivakumar, S. Sheeja, M.P. Kurup, E.R. Tiekink, Inorg. Chim. Acta 362 (2009) 4191–4197.
[4] R. Krishnan, J. Thirumalai, A. Kathiravan, Electron. Mater. Lett. 11 (2015) 24–33.
[5] N. Hildebrandt, H.-G. Lohmannsroben, Curr. Chem. Biol. 1 (2007) 167–186.
[6] A. Valore, E. Cariati, S. Righetto, D. Roberto, F. Tessore, R. Ugo, I.L. Fragala, M.E. Fragala, G. Malandrino, F. De Angelis, J. Am. Chem. Soc. 132 (2010) 4966–4970.
[7] J.P. Morrall, G.T. Dalton, M.G. Humphrey, M. Samoc, Adv. Organomet. Chem. 55 (2007) 61–136.
[8] S.M. Cornet, I. May, M.P. Redmond, A.J. Selvage, C.A. Sharrad, O. Rosnel, Polyhedron 28 (2009) 363–369.
[9] Y. Zhang, I. Karatchevtseva, J.R. Price, I. Aharonovich, F. Kadi, G.R. Lumpkin, F. Li, RSC Adv. 5 (2015) 33249–33253.
[10] H. Moll, A. Rossberg, R. Steudtner, B.R. Drobot, K. Müller, S. Tsushima, Inorg. Chem. 53 (2014) 1585–1593.
[11] J.D. Van Horn, H. Huang, Coord. Chem. Rev. 250 (2006) 765–775.
[12] A.E. Gorden, J. Xu, K.N. Raymond, P. Durbin, Chem. Rev. 103 (2003) 4207–4282.
[13] W. Stevens, F. Bruenger, D. Atherton, J. Smith, G. Taylor, Radiat. Res. 83 (1980) 109–126.
[14] S. Scapolan, E. Ansorborlo, C. Moulin, C. Madic, Radiat. Prot. Dosim. 79 (1998) 505–508.
[15] C. Vidaud, A. Dedieu, C. Basset, S. Plantevin, I. Dany, O. Pible, E. Quéméneur, Chem. Res. Toxicol. 18 (2005) 946–953.
[16] C. Vidaud, S. Gourion-Arsiquaud, F. Rollin-Genetet, C. Torne-Celer, S. Plantevin, O. Pible, C. Berthomieu, E. Quéméneur, Biochemistry 46 (2007) 2215–2226.
[17] H. Huang, S. Chaudhary, J.D. Van Horn, Inorg. Chem. 44 (2005) 813–815.
[18] M. Sutton, S.R. Burastero, Chem. Res. Toxicol. 17 (2004) 1468–1480.
[19] B.C. Baguley, D.J. Kerr, Anticancer Drug Development, Academic Press, 2001.
[20] H. Vogel, Drug Discovery and Evaluation: Pharmacological AssaysSpringer Science & Business Media 2007.
[21] W.P. Roos, B. Kaina, Trends Mol. Med. 12 (2006) 440–450.
[22] J.B. Chaires, Curr. Opin. Struct. Biol. 8 (1998) 314–320.
[23] S.Y. Ebrahimipour, H. Khabazadeh, J. Castro, I. Sheikhshoaie, A. Crochet, K.M. Fromm, Inorg. Chim. Acta 427 (2015) 52–61.
[24] A. Bruker, Smart, Saint, Bruker AXS Inc., Madison, Wisconsin, USA, 2007.
[25] P. McArdle, J. Appl. Crystallogr. 28 (1995) 65.
[26] G.M. Sheldrick, Acta Crystallogr. Sect. A: Found. Crystallogr. 64 (2007) 112–122.
[27] F. Arjmand, M. Aziz, Eur. J. Med. Chem. 44 (2009) 834–844.
[28] O. Trott, A.J. Olson, J. Comput. Chem. 31 (2010) 455–461.
[29] S.Y. Ebrahimipour, Z.R. Ranjabr, E.T. Kermani, B.P. Amiri, H.A. Rudbari, A. Saccá, F. Hoseinzade, Transit. Met. Chem. 40 (2015) 39–45.
[30] S.Y. Ebrahimipour, I. Sheikhshoaie, A. Crochet, M. Khaleghi, K.M. Fromm, J. Mol. Struct. 1072 (2014) 267–276.

[31] S. Yousef Ebrahimipour, M. Mohamadi, J. Castro, N. Mollania, H. Amiri Rudbari, A. Saccá, J. Coord. Chem. 68 (2015) 632–649.
[32] S. Ebrahimipour, I. Sheikhshoaie, J. Castro, M. Dusek, Z. Tohidiyan, V. Eigner, RSC Adv. 5 (2015) 95104–95117.
[33] S.Y. Ebrahimipour, I. Sheikhshoaie, M. Mohamadi, S. Suarez, R. Baggio, M. Khaleghi, M. Torkzadeh-Mahani, A. Mostafavi, Spectrochim. Acta A 142 (2015) 410–422.
[34] M. Azam, S.I. Al-Resayes, G. Velmurugan, P. Venuvanalingam, J. Wagler, E. Kroke, Dalton Trans. 44 (2015) 568–577.
[35] R. Takjoo, S.W. Ng, E.R. Tiekink, Acta Crystallogr. Sect. E: Struct. Rep. Online 68 (2012) m244–m245.
[36] C. Gatto, E. Schulz Lang, A. Kupfer, A. Hagenbach, U. Abram, Z. Anorg. Allg. Chem. 630 (2004) 1286–1295.
[37] D.F. Back, G.M. de Oliveira, D. Roman, M.A. Ballin, R. Kober, P.C. Piquini, Inorg. Chim. Acta 412 (2014) 6–14.
[38] K.C. Skyrianou, V. Psycharis, C.P. Raptopoulou, D.P. Kessissoglou, G. Psomas, J. Inorg. Biochem. 105 (2011) 63–74.
[39] A. Silvestri, G. Barone, G. Ruisi, D. Anselmo, S. Riela, V.T. Liveri, J. Inorg. Biochem. 101 (2007) 841–848.
[40] J.-Q. Sha, X. Li, H.-B. Qiu, Y.-H. Zhang, H. Yan, Inorg. Chim. Acta 383 (2012) 178–184.
[41] M. Navarro, E.J. Cisneros-Fajardo, A. Sierralta, M. Fernández-Mestre, P. Silva, D. Arrieche, E. Marchán, JBIC, J. Biol. Inorg. Chem. 8 (2003) 401–408.
[42] A. Terenzi, G. Barone, A. Silvestri, A.M. Giuliani, A. Ruggirello, V.T. Liveri, J. Inorg. Biochem. 103 (2009) 1–9.
[43] M. Mohamadi, S.Y. Ebrahimipour, M. Torkzadeh-Mahani, S. Foro, A. Akbari, RSC Adv. 5 (2015) 101063–101075.
[44] M.T. Carter, M. Rodriguez, A.J. Bard, J. Am. Chem. Soc. 111 (1989) 8901–8911.
[45] M.R. Eftink, C.A. Ghiron, Anal. Biochem. 114 (1981) 199–227.
[46] G. Zhang, Y. Ma, L. Wang, Y. Zhang, J. Zhou, Food Chem. 133 (2012) 264–270.
[47] J. Zhu, L. Wu, Q. Zhang, X. Chen, X. Liu, Spectrochim. Acta A 95 (2012) 252–257.
[48] D. Lu, X. Zhao, Y. Zhao, B. Zhang, B. Zhang, M. Geng, R. Liu, Food Chem. Toxicol. 49 (2011) 3158–3164.
[49] Y. Chen, M.-Y. Qin, J.-H. Wu, L. Wang, H. Chao, L.-N. Ji, A.-L. Xu, Eur. J. Med. Chem. 70 (2013) 120–129.
[50] N. Desbois, D. Pertuit, J. Moretto, C. Cachia, B. Chauffert, F. Bouyer, Eur. J. Med. Chem. 69 (2013) 719–727.